

## **Supporting Information**

### **Circularly Polarized Luminescence from Decamethylcurbit[5]uril-triggered Chiral Supramolecular Hydrogels**

Bing An, Qingmei Ge, Hang Cong\*, Ruihan Gao\*

Key Laboratory of Macrocyclic and Supramolecular Chemistry of Guizhou Province, Guizhou University, Guiyang, 550025, China. Email: [hcong@gzu.edu.cn](mailto:hcong@gzu.edu.cn)

#### 1 Materials

Demethylcurbit[5]uril (Me<sub>10</sub>Q[5]) was synthesized according to the literature procedure.<sup>1</sup> Other reagents and chemicals were obtained in analytical reagent grade from Innochem Co., Ltd (Beijing, China) and Shanghai Aladdin Biochemical Technology Co., Ltd. (Shanghai, China), which were used without further purification. The (*R/S*)-2,2'-diamino-1,1'-binaphthalene hydrochloride ((*R/S*)-BINAM) was prepared by dissolving (*R/S*)-2,2'-diamino-1,1'-binaphthalene in 6 M HCl following by freeze-drying. Double distilled water was used throughout.

#### 2 Experimental Instruments and Methods

The Me<sub>10</sub>Q[5]/(*R/S*)-BINAM co-assembled hydrogels were prepared by mixture of severally heating and dissolving Me<sub>10</sub>Q[5] and (*R/S*)-BINAM in H<sub>2</sub>O. <sup>1</sup>H NMR spectra were recorded at 20 °C on a JEOL JNM-ECZ400s spectrometer in D<sub>2</sub>O. The association constants of the host-guest interactions were calculated by nonlinear fitting employing the Equation (S1):

$$\Delta\delta = \frac{\Delta\varepsilon_1 K_{a1} [H_0][G_0] + \Delta\varepsilon_2 K_{a1} K_{a2} [G_0][H_0]^2}{1 + K_{a1} [H_0] + K_{a1} K_{a2} [H_0]^2} \quad (\text{S1})$$

DOSY spectra were recorded at room temperature on a JEOL JNM-ECZ400s spectrometer in D<sub>2</sub>O UV-visible (UV-Vis) absorption spectra of the guest and the host-guest complex were recorded on a UV-2700 spectrophotometer (Shimadzu Instruments Co. Ltd.) at 25 °C. The Job's plot of (*R/S*)-BINAM with Me<sub>10</sub>Q[5] was obtained by preparing a series of host-guest solutions with a total concentration of  $C_{(R/S)\text{-BINAM}} + C_{\text{Me}_{10}\text{Q}[5]} = 10 \mu\text{M}$ . A range of solutions was prepared by varying the molar ratio of the two components, resulting in Me<sub>10</sub>Q[5] concentration combinations of 0:10, 1:9, 2:8, 3:7, 4:6, up to 10:0. The UV-Vis spectrophotometric titrations were carried out at  $\lambda_{\text{max}} = 235 \text{ nm}$ . An aqueous solution of (*R/S*)-BINAM was prepared with a concentration of 10  $\mu\text{M}$ , this solution was combined with Me<sub>10</sub>Q[5] to give a  $C_{\text{Me}_{10}\text{Q}[5]}/C_{(R/S)\text{-BINAM}}$  ratio of 0, 1:10, 1:5, 3:10, 2:5, 1:2, and 1:1 and so on. The association constants of the host-guest interactions were calculated by nonlinear fitting employing the Equation (S2):

$$\Delta A = \frac{\Delta\varepsilon_1 K_{a1} [H_0][G_0] + \Delta\varepsilon_2 K_{a1} K_{a2} [G_0][H_0]^2}{1 + K_{a1} [H_0] + K_{a1} K_{a2} [H_0]^2} \quad (S2)$$

Dynamic light scattering (DLS) analysis was conducted on a laser light scattering spectrometer (BI-200SM) equipped with a digital correlator (BI-9000AT) at 25 °C. SEM observations were carried out using a ZEISS Sigma field emission SEM system. Samples were deposited on a SiO<sub>2</sub>/Si substrate, and then lyophilized or dried at room temperature. Dynamic oscillatory rheological characterization was performed with an Ares G2 (TA Instruments, USA) controlled strain rheometer at 25 °C. Fluorescence spectra were recorded on a Shimadzu RF-6000 Fluorescence Spectrophotometer (Shimadzu, Japan). The CD and CPL spectra of the Me<sub>10</sub>Q[5]/(R/S)-BINAM hydrogel system were measured on a Circular dichroism spectrometer (Applied photophysics Chirascan) and JASCO CPL-300 spectrometer at room temperature, respectively. The fluorescence quantum yield was measured using Absolute PL quantum yield spectrometer C11347, equipped with a 150W steady-state xenon lamp. Fluorescence lifetime testing was conducted using the high-precision TAUC11367 fluorescence lifetime measurement instrument, equipped with a nanosecond pulsed LED light source. The structures were optimized at the B3LYP/6-31+G\* (d,p) level of theory with the Gaussian 16 software package.<sup>2</sup> The binding energy ( $E_{\text{binding}}$ ) can be defined as the difference between the total energy of the host-guest complex and the sum of the total energies of the separated host and guest molecules. It is typically represented by the Equation (S3)<sup>3</sup>:

$$E_{\text{binding}} = E_{\text{host-guest complex}} - (E_{\text{host}} + E_{\text{guest}}) \quad (S3)$$

where:

$E_{\text{host-guest complex}}$  is the total energy of the host-guest complex,  $E_{\text{host}}$  is the total energy of the host molecule,  $E_{\text{guest}}$  is the total energy of the guest molecule.

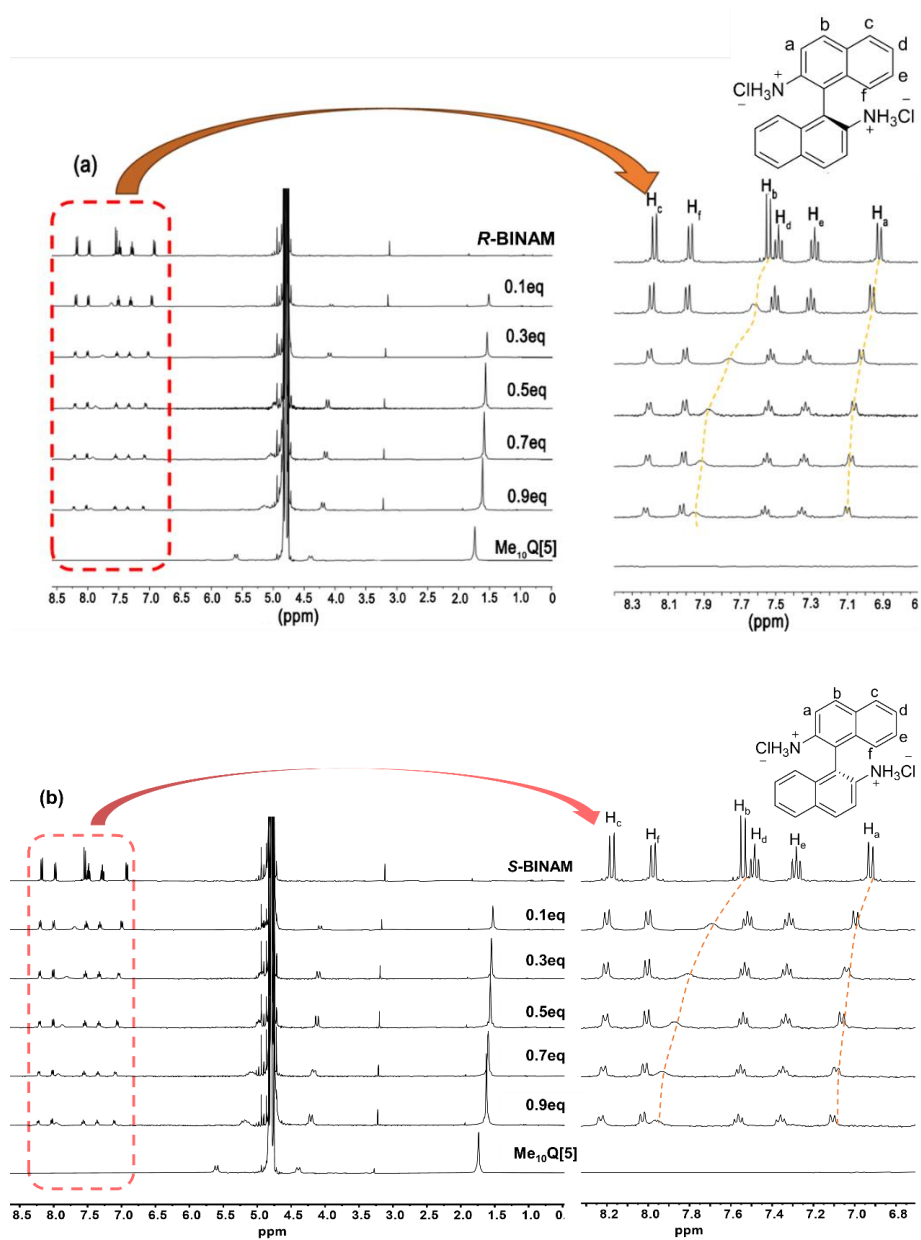


**Fig. S1**  $^1\text{H}$  NMR spectra of (a) *R*-BINAM, (b) *S*-BINAM upon addition of molar equivalents of  $\text{Me}_{10}\text{Q}[5]$ : 0.1eq-0.9eq (5 mM (*R/S*)-BINAM in aqueous solution, 400 MHz)

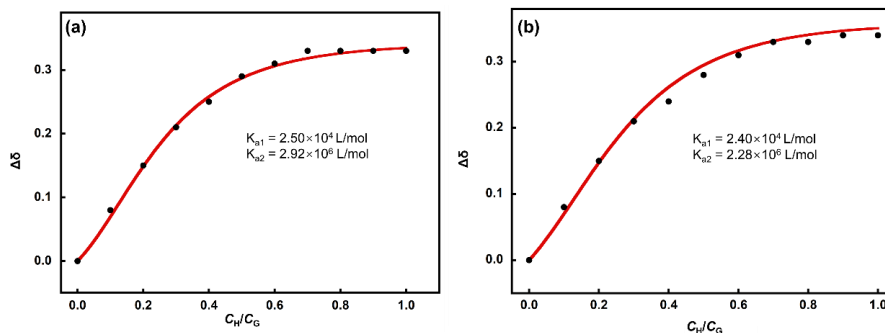


**Fig. S2.**  $^1\text{H}$  NMR titrations of (a) *R*-BINAM, (b) *S*-BINAM with  $\text{Me}_{10}\text{Q}[5]$  (the concentration of (*R/S*)-BINAM was fixed to 10 mM in aqueous solution)

The first-order and second-order association constants for the supramolecular interactions were determined by curve-fitting the proton resonance chemical shift changes ( $\Delta\delta$ ) using Equation (S1), which were found to be  $K_{a1} = 2.50 \times 10^4$  L/mol and  $K_{a2} = 2.92 \times 10^6$  L/mol for *R*-BINAM and  $\text{Me}_{10}\text{Q}[5]$ ,  $K_{a1} = 2.40 \times 10^4$  L/mol and  $K_{a2} = 2.28 \times 10^6$  L/mol for *S*-BINAM and  $\text{Me}_{10}\text{Q}[5]$ , respectively.

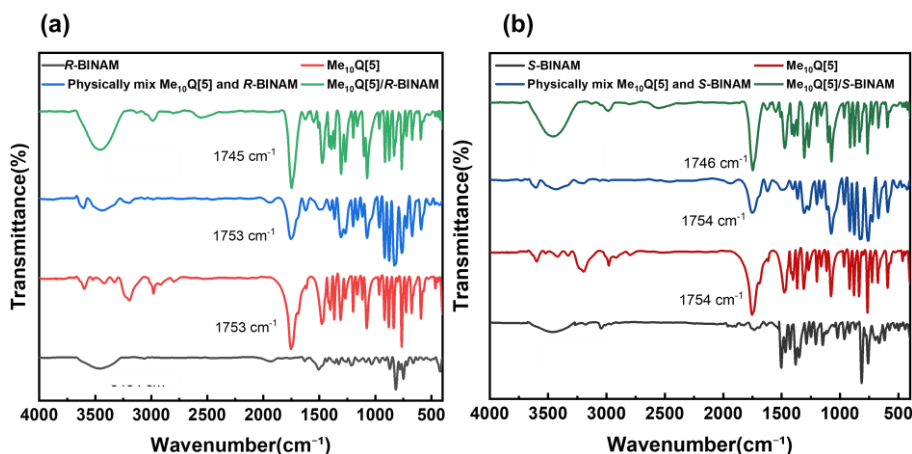


**Fig. S3** FT-IR absorbance spectra of (a)  $\text{Me}_{10}\text{Q}[5]/R\text{-BINAM}$ ; (b)  $\text{Me}_{10}\text{Q}[5]/S\text{-BINAM}$ . black curve: BINAM; red curve:  $\text{Me}_{10}\text{Q}[5]$ ; blue curve: physically mix  $\text{Me}_{10}\text{Q}[5]$  and (*R/S*)-BINAM; green curve:  $\text{Me}_{10}\text{Q}[5]/(R/S)\text{-BINAM}$ .

The supramolecular assemblies between  $\text{Me}_{10}\text{Q}[5]$  and (*R/S*)-BINAM were evidenced with FT-IR. The C=O stretching vibration of  $\text{Me}_{10}\text{Q}[5]$  shifted from  $1753\text{ cm}^{-1}$  to  $1745\text{ cm}^{-1}$  in  $\text{Me}_{10}\text{Q}[5]/R\text{-BINAM}$  spectra. Similarly, in the  $\text{Me}_{10}\text{Q}[5]/S\text{-BINAM}$  spectra, the C=O stretching vibration of  $\text{Me}_{10}\text{Q}[5]$  shifted from  $1754\text{ cm}^{-1}$  to  $1746\text{ cm}^{-1}$ . The above shifts suggested the supramolecular interactions between the carbonyl groups of  $\text{Me}_{10}\text{Q}[5]$  and (*R/S*)-BINAM.

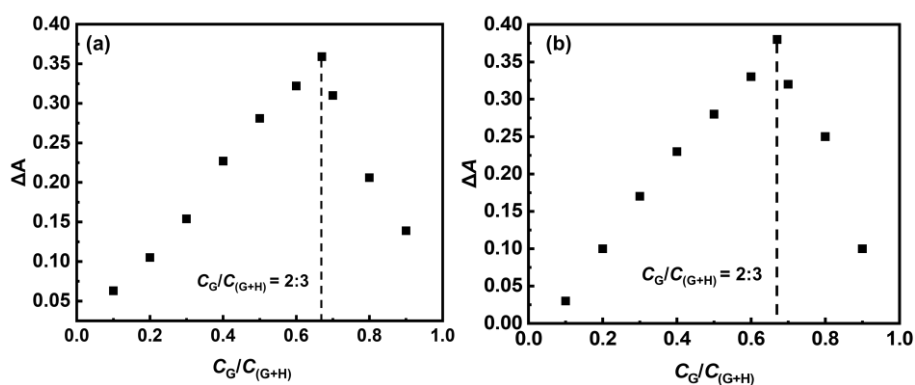


**Fig. S4.** Job's plots of (a) *R*-BINAM, (b) *S*-BINAM with Me<sub>10</sub>Q[5] (UV-visible absorbance at 237 nm with  $C_{(R/S)\text{-BINAM}} + C_{\text{Me}_{10}\text{Q}[5]} = 10 \mu\text{M}$  in aqueous solution)

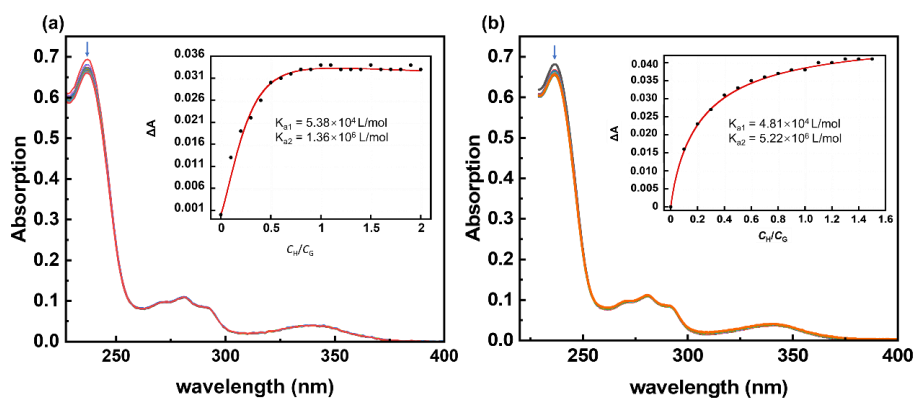


**Fig. S5.** UV-vis absorption spectral titrations of (a) *R*-BINAM, (b) *S*-BINAM with Me<sub>10</sub>Q[5] (the concentration of (*R/S*)-BINAM was fixed to 10  $\mu\text{M}$  in aqueous solution)

The (*R/S*)-BINAM solution produced three absorption peaks at 235 nm, 285 nm, and 340 nm, respectively, corresponding to the E<sub>1</sub>, E<sub>2</sub>, and B bands of the aromatic rings of binaphthyl groups. With the incremental addition of Me<sub>10</sub>Q[5] at varying molar ratios, the absorption band at 235 nm progressively decreased, while the absorption intensity kept a constant at the 1:2 molar ratio of Me<sub>10</sub>Q[5] to (*R/S*)-BINAM. The first-order and second-order association constants for the supramolecular interaction were determined with curve-fitting of the absorption values with Equation (S2), which were found to be  $K_{a1} = 5.38 \times 10^4 \text{ L/mol}$  and  $K_{a2} = 1.36 \times 10^6 \text{ L/mol}$ , for *R*-BINAM and Me<sub>10</sub>Q[5],  $K_{a1} = 4.81 \times 10^4 \text{ L/mol}$  and  $K_{a2} = 5.22 \times 10^6 \text{ L/mol}$  for *S*-BINAM and Me<sub>10</sub>Q[5], respectively. The values are within the same order of magnitude as the binding constants determined by <sup>1</sup>H NMR titration.

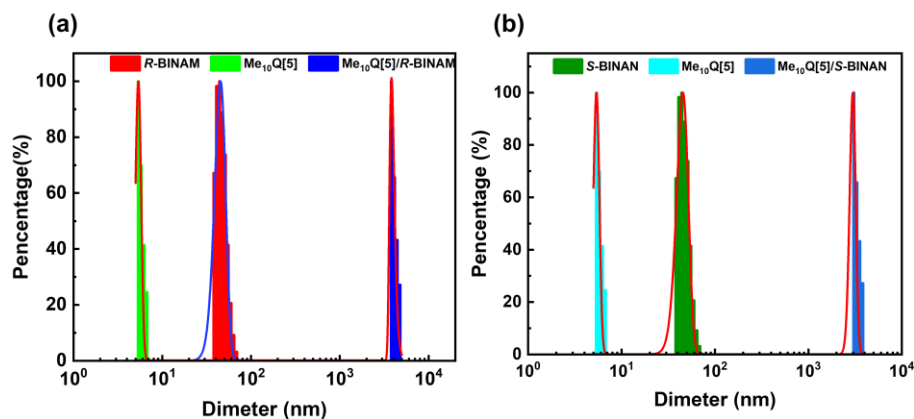


**Fig. S6.** DLS of (a) Me<sub>10</sub>Q[5]/*R*-BINAM assemblies (The green bar represents 0.5 mM Me<sub>10</sub>Q[5] in H<sub>2</sub>O, the red bar represents 1.0 mM *R*-BINAM in H<sub>2</sub>O, and the blue bar represents a mixture of 0.5 mM Me<sub>10</sub>Q[5] and 1.0 mM *R*-BINAM in H<sub>2</sub>O.) ; (b) Me<sub>10</sub>Q[5]/*S*-BINAM. (The cyan bar represents 0.5 mM Me<sub>10</sub>Q[5] in H<sub>2</sub>O, the green bar represents 1.0 mM *S*-BINAM in H<sub>2</sub>O, and the blue bar represents a mixture of 0.5 mM Me<sub>10</sub>Q[5] and 1.0 mM *S*-BINAM in H<sub>2</sub>O.)

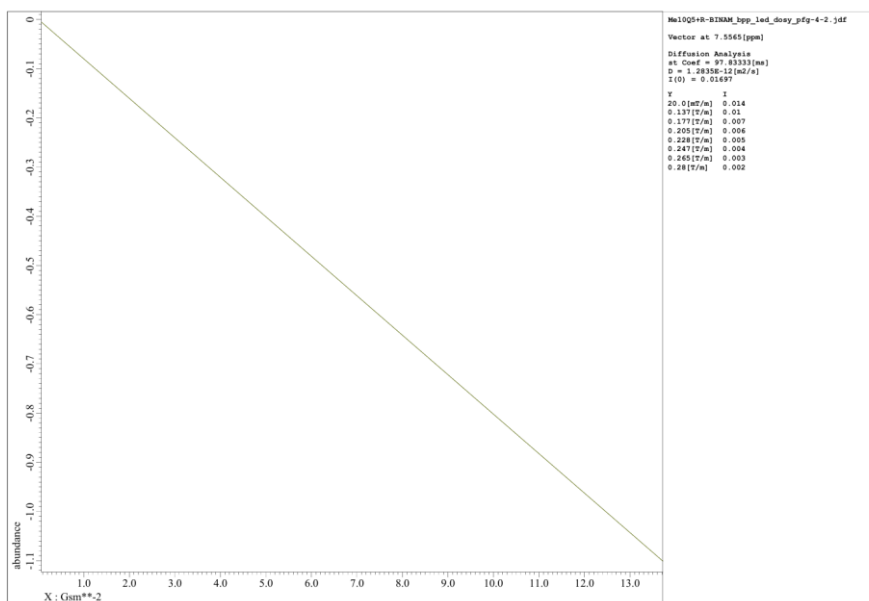


**Fig. S7** DOSY spectrum of Me<sub>10</sub>Q[5]/*R*-BINAM (25°C, a mixture of  $1.0 \times 10^{-3}$  M Me<sub>10</sub>Q[5] and  $2.0 \times 10^{-3}$  M *R*-BINAM in D<sub>2</sub>O)

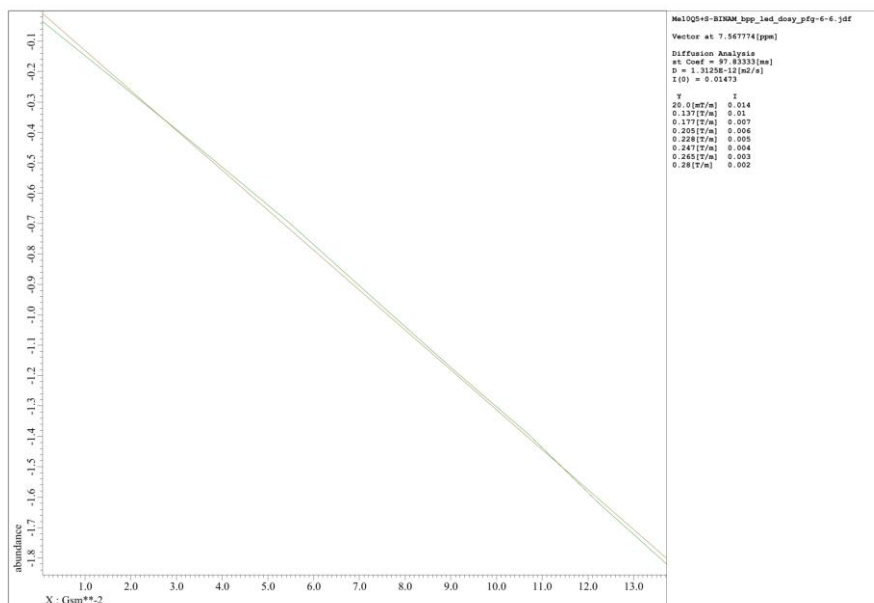


**Fig. S8** DOSY spectrum of Me<sub>10</sub>Q[5]/S-BINAM(25°C, a mixture of 1.0×10<sup>-3</sup>M Me<sub>10</sub>Q[5] and 2.0×10<sup>-3</sup>M S-BINAM in D<sub>2</sub>O)

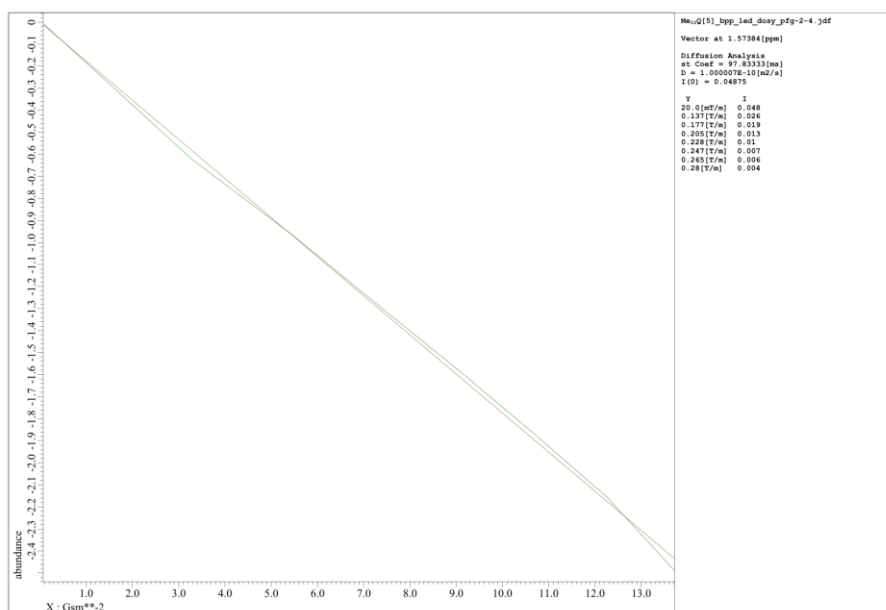


**Fig. S9** DOSY spectrum of Me<sub>10</sub>Q[5] (25°C, 1×10<sup>-3</sup>M in D<sub>2</sub>O).

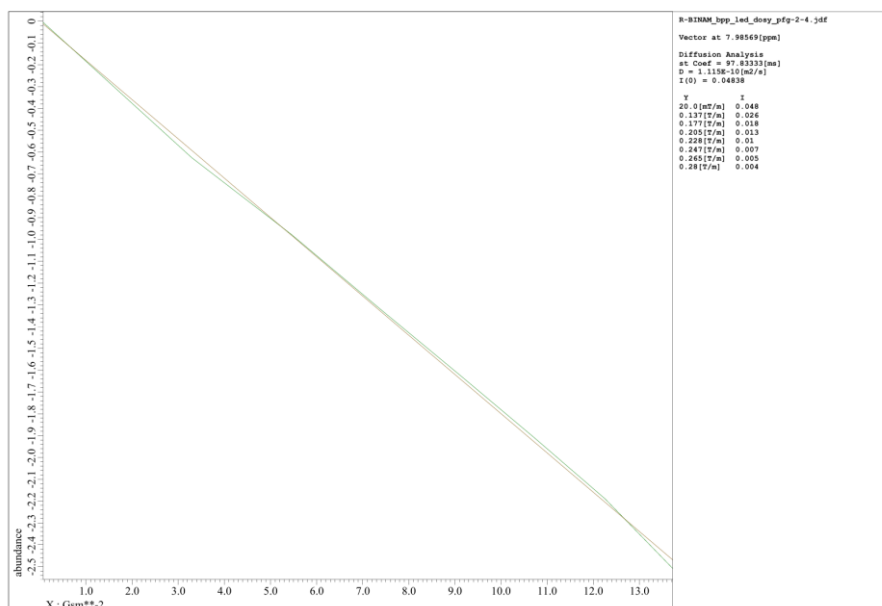


**Fig. S10** DOSY spectrum of *R*-BINAM (25°C,  $2 \times 10^{-3}$ M in D<sub>2</sub>O).

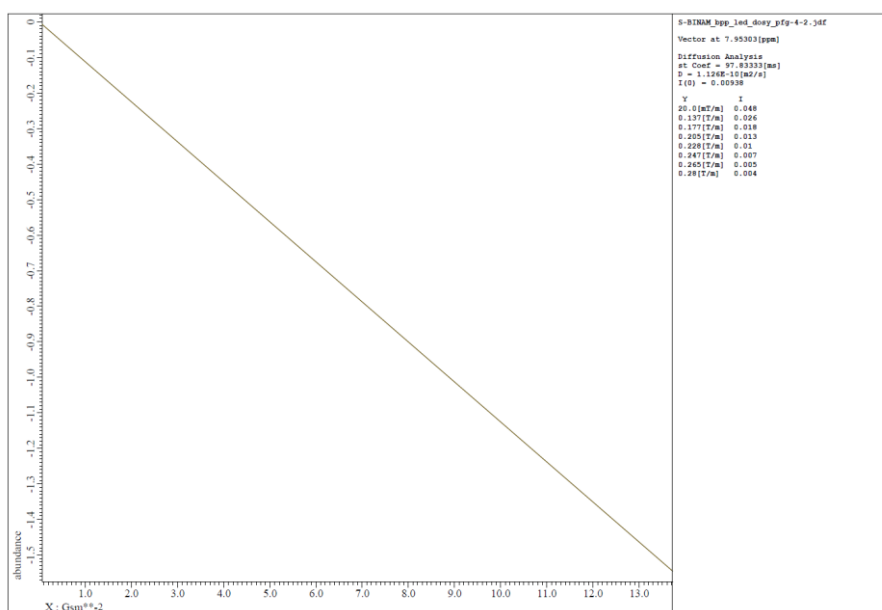


**Fig. S11** DOSY spectrum of *S*-BINAM (25°C,  $2 \times 10^{-3}$ M in D<sub>2</sub>O).

Diffusion ordered spectroscopy (DOSY) experiments were performed on Me<sub>10</sub>Q[5], (*R/S*)-BINAM, and their supramolecular assemblies at room temperature. The diffusion coefficient of Me<sub>10</sub>Q[5] was  $D = 1.000007 \times 10^{-10}$  [m<sup>2</sup>/s], and the diffusion coefficients of (*R/S*)-BINAM were  $D = 1.115 \times 10^{-10}$  [m<sup>2</sup>/s] and  $D = 1.126 \times 10^{-10}$  [m<sup>2</sup>/s]. The values were detected to be  $D = 1.12835 \times 10^{-12}$  [m<sup>2</sup>/s] for *R*-BINAM/Me<sub>10</sub>Q[5] and  $D = 1.3125 \times 10^{-12}$  [m<sup>2</sup>/s] for *S*-BINAM/Me<sub>10</sub>Q[5], respectively. The results revealed the decrease in apparent diffusion coefficient for the molecular expansion in the supramolecular systems, which confirmed the host-guest interactions.

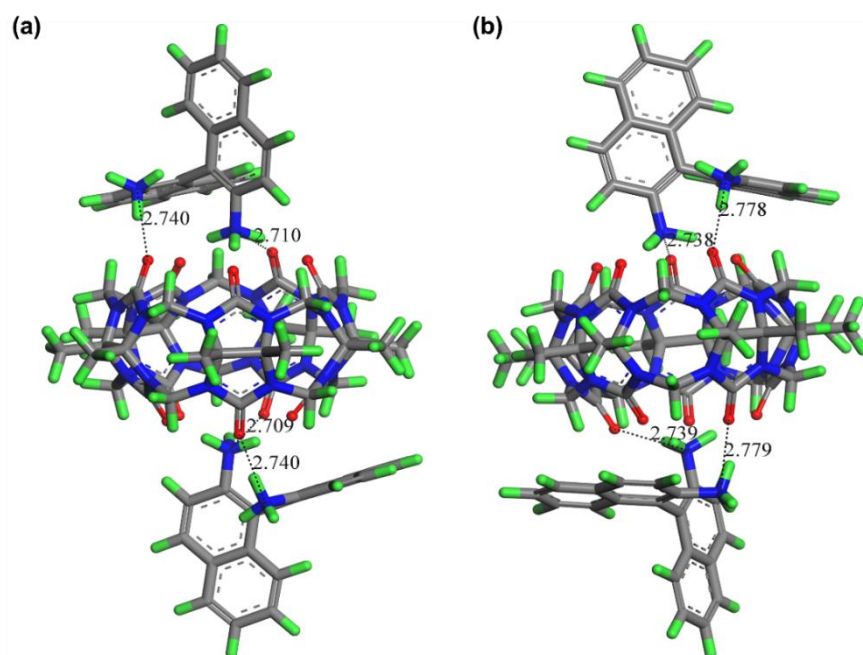


**Fig. S12** Computational calculations for two assemble modes of Me<sub>10</sub>Q[5]/(*R/S*)-BINAM: (a) Me<sub>10</sub>Q[5]/*R*-BINAM (b) Me<sub>10</sub>Q[5]/*S*-BINAM

The simulated geometries of the host-guest interactions between Me<sub>10</sub>Q[5] and (*R/S*)-BINAM were provided to understand what the static structures look like and their thermodynamic stability. The optimized 1:2 complexes of Me<sub>10</sub>Q[5] with (*R/S*)-BINAM show hydrogen bonding between the carbonyl groups of Me<sub>10</sub>Q[5] and the two amino groups of (*R/S*)-BINAM, one at the portal center and the other at its edge, with interaction distances between the carbonyl oxygen atoms and amino nitrogen atoms ranging from 2.7 to 2.8 Å. Binding energies were calculated as -124.31 kcal/mol for Me<sub>10</sub>Q[5]/*S*-BINAM and -126.90 kcal/mol for Me<sub>10</sub>Q[5]/*R*-BINAM, showing similar stability for both enantiomers and indistinguishable assembly processes.

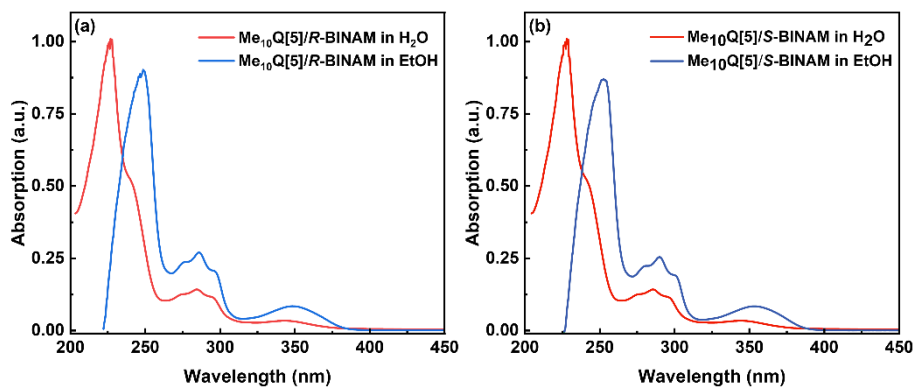


**Fig. S13** UV-Vis absorption spectrum of (a) Me<sub>10</sub>Q[5]/R-BINAM assembly; (b) Me<sub>10</sub>Q[5]/S-BINAM assembly. (Red line: Me<sub>10</sub>Q[5]/(R/S)-BINAM assembly in H<sub>2</sub>O containing 10 μM Me<sub>10</sub>Q[5] and 20 μM (R/S)-BINAM; blue line: Me<sub>10</sub>Q[5]/(R/S)-BINAM assembly in EtOH containing 10 μM Me<sub>10</sub>Q[5] and 20 μM (R/S)-BINAM.)

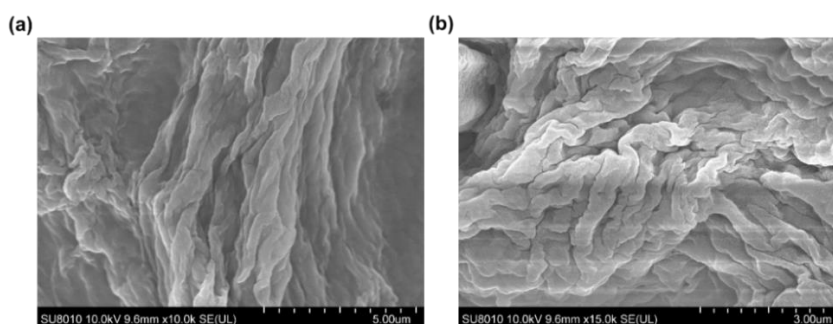


**Fig. S14** SEM images of the (a) Me<sub>10</sub>Q[5]/R-BINAM co-assembled hydrogel; (b) Me<sub>10</sub>Q[5]/S-BINAM co-assembled hydrogel

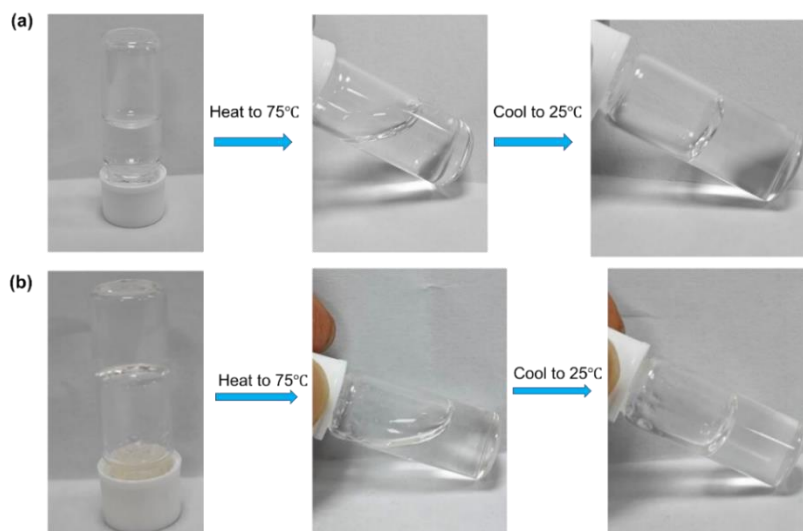


**Fig. S15** Sol-gel phase transition of the (a) R-hydrogel; (b) S-hydrogel

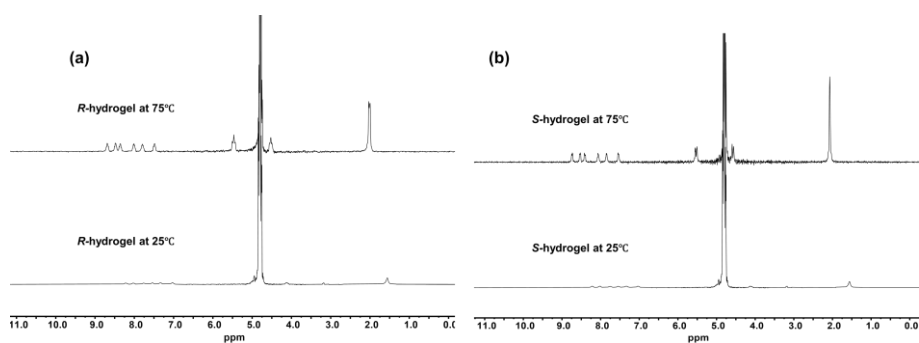


**Fig. S16**  $^1\text{H}$  NMR spectra of (a) *R*-hydrogel; (b) *S*-hydrogel at different temperatures.

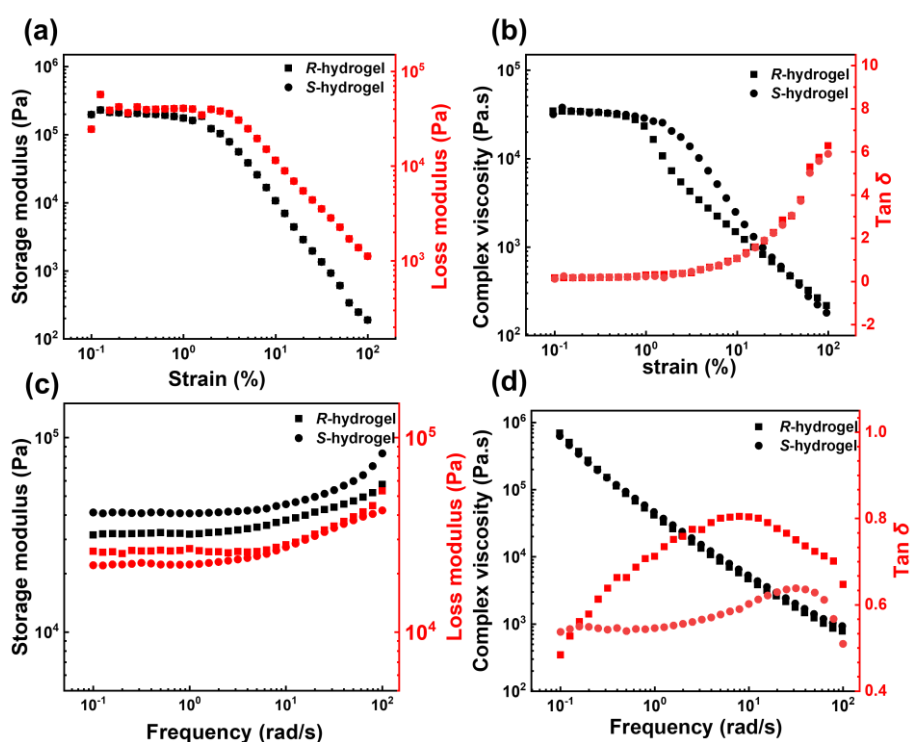


**Fig. S17** Dynamic oscillatory rheological characterizations of (*R/S*)-hydrogels were conducted at 25 °C: (a) storage and loss modulus obtained from the strain amplitude sweep measurements; (b) complex viscosity and  $\tan \delta$  obtained from the strain amplitude sweep measurements; (c) storage and loss modulus obtained from the frequency sweep measurements; (d) complex viscosity and  $\tan \delta$  obtained from the frequency sweep measurements.

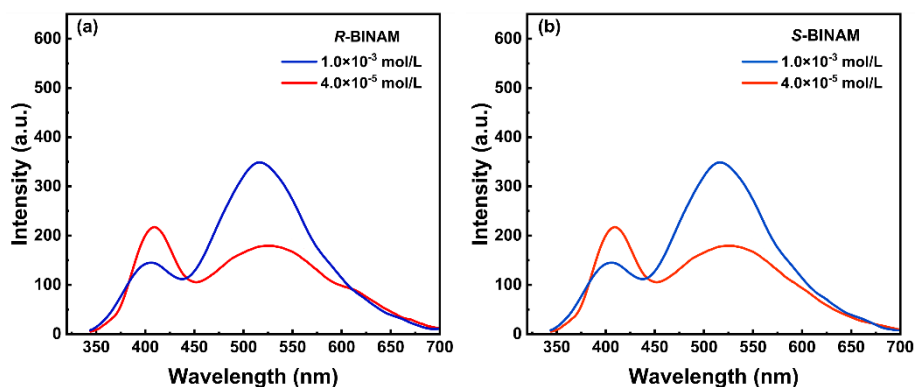


**Fig. S18** The fluorescence emission of (*R/S*)-BINAM in dilute solutions with different concentrations. Blue line: in aqueous solution of  $1.0 \times 10^{-3}$  M (*R/S*)-BINAM; red line: in aqueous solution of  $4.0 \times 10^{-5}$  M (*R/S*)-BINAM.

As the concentration increased, the fluorescence intensity at 520 nm was stronger, and the emission at 400 nm were weakened, which suggested molecular aggregation to form dimers at higher concentration, and therefore, the emission at 400 nm was assigned to the monomer, while the emission at 520 nm should be produced by the dimer.

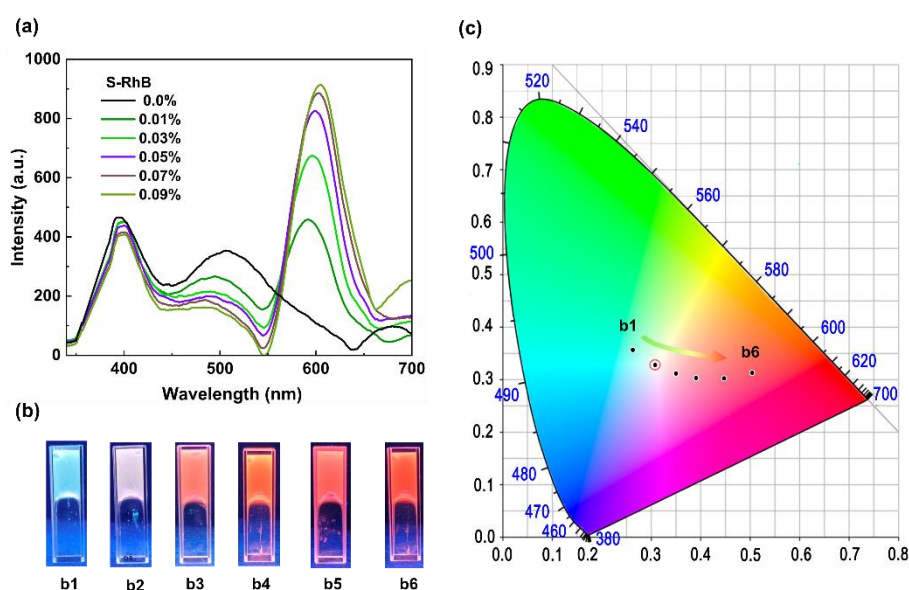


**Fig. S19** (a) Fluorescence spectra and of *S*-hydrogel in the presence of different amounts of S-RhB (b) CIE coordinate (c) the gel color change under UV light irradiation ((a) 0% to 0.09% corresponds to b1 to b6 in (b) and (c))

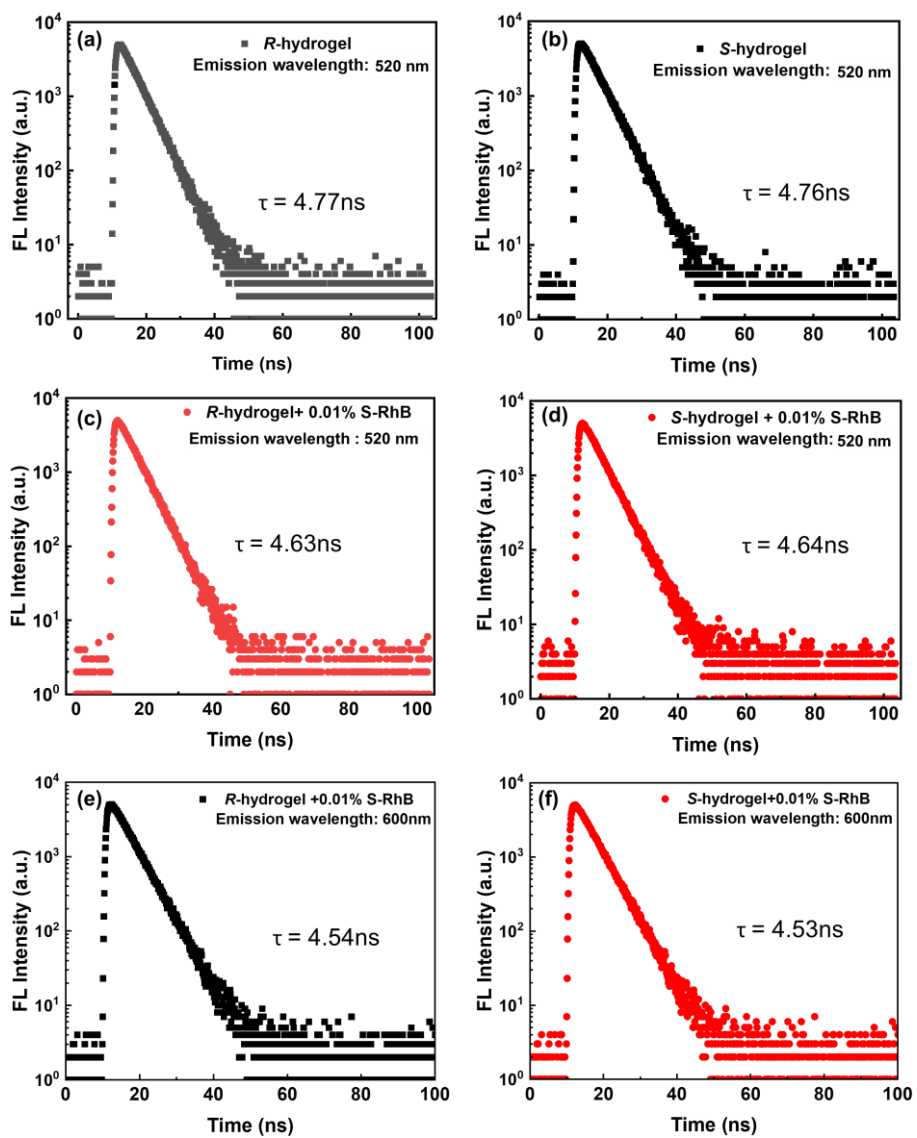


**Fig. S20** Emission decay curves of (*R/S*)-hydrogel, (*R/S*)-hydrogel+0.01% S-RhB at emission wavelengths of 520 nm ((a)-(d)) and 600 nm ((e)-(f)).

**Table S1** PLQY ( $\Phi$ ) and Fluorescence lifetime ( $\tau$ ) of (*R/S*)-hydrogels doped and undoped with 0.01% S-RhB (Ex = 340nm)

	$\phi$ (%) Em=520nm	$\phi$ (%) Em=600nm	$\tau$ (ns) Em=520nm	$\tau$ (ns) Em=600nm
<i>R</i> -hydrogel	3.6%	-	4.77	-
<i>R</i> -hydrogel +0.01% S-RhB	2.4%	1.2%	4.63	4.54
<i>S</i> -hydrogel	3.7%	-	4.76	-
<i>S</i> -hydrogel +0.01% S-RhB	2.5%	1.2%	4.64	4.53

S1 Flinn, A.; Hough, G. C.; Stoddart, J. F.; Williams, D. J., *Angew. Chem. Int. Ed* 1992, **31** (11), 1475-1477.

S2 Frisch, M. J.; Trucks, G. W.; Schlegel, H. B.; Scuseria, G. E.; Robb, M. A.; Cheeseman, J. R.; Scalmani, G.; Barone, V.; Petersson, G. A.; Nakatsuji, H.; Li, X.; Caricato, M.; Marenich, A. V.; Bloino, J.; Janesko, B. G.; Gomperts, R.; Mennucci, B.; Hratchian, H. P.; Ortiz, J. V.; Izmaylov, A. F.; Sonnenberg, J. L.; Williams, D.; Ding, F.; Lipparini, F.; Egidi, F.; Goings, J.; Peng, B.; Petrone, A.; Henderson, T.; Ranasinghe, D.; Zakrzewski, V. G.; Gao, J.; Rega, N.; Zheng, G.; Liang, W.; Hada, M.; Ehara, M.; Toyota, K.; Fukuda, R.; Hasegawa, J.; Ishida, M.; Nakajima, T.; Honda, Y.; Kitao, O.; Nakai, H.; Vreven, T.; Throssell, K.; Montgomery Jr., J. A.; Peralta, J. E.; Ogliaro, F.; Bearpark, M. J.; Heyd, J. J.; Brothers, E. N.; Kudin, K. N.; Staroverov, V. N.; Keith, T. A.; Kobayashi, R.; Normand, J.; Raghavachari, K.; Rendell, A. P.; Burant, J. C.; Iyengar, S. S.; Tomasi, J.; Cossi, M.; Millam, J. M.; Klene, M.; Adamo, C.; Cammi, R.; Ochterski, J. W.; Martin, R. L.; Morokuma, K.; Farkas, O.; Foresman, J. B.; Fox, D. J. *Gaussian 16 Rev. C.01*, Gaussian, Inc.: Wallingford, CT, 2016.

S3 Albdallah, S. K.; Assaf, K. I.; Bodoor, K.; Al-Sakhen, N. A.; Malhis, L. D.; Alhmaideen, A. I.; El-Barghouthi, M. I., *J. Solution Chem.* 2018, **47** (11), 1768-1778.